Scientia Iranica (2024) 31(2), 137–148

Sharif University of Technology
Scientia Iranica
Transactions D: Computer Science & Engineering and Electrical Engineering
https://scientiairanica.sharif.edu

TDE based model-free control for rigid robotic manipulators under nonlinear friction

S. Ahmed[a,*], I. Ghous[b], and F. Mumtaz[a]

a. *Department of Mechatronics, SZABIST, Karachi, Pakistan.*
b. *Department of Electrical and Computer Engineering, COMSATS University, Lahore, Pakistan.*

Received 29 November 2020; received in revised form 18 January 2022; accepted 18 April 2022

KEYWORDS
Model-free control;
Time delay estimation;
Sliding mode control;
Stribeck friction;
Robotic manipulators.

Abstract. This paper establishes a model-free finite-time tracking control of nonlinear robotic manipulator systems. The proposed controller incorporates both Time Delay Estimation (TDE) and an enhanced Terminal Sliding Mode Control (TSMC). The improved TSMC scheme is devised using Fractional-Order TSMC (FOTSMC) and Proportional-Integral-Derivative (PID) control to obtain robust tracking and high control performance. The TDE is designed to estimate the unknown nonlinear dynamics of robotic manipulators, including the Stribeck friction and the external disturbances. Due to Stribeck friction, the effect of TDE error may fail to obtain the desired error performance; thus, another TDE loop is devised to compensate for TDE error generated by non-smooth frictions. The Lyapunov criterion is used to investigate the finite-time stability to analyze the behavior of the designed approach. Finally, computer simulations of the proposed method on PUMA 560 robotic manipulators are performed in contrast with FOTSMC and Adaptive Fractional-Order Nonsingular Terminal Sliding Mode Control (AFONTSMC).

1. Introduction

A robotic manipulator is a nonlinear mechanical device and is generally used in processing/manufacturing industries and its applications because it is cost-effective and replaces manual labor for complicated and repetitive tasks [1–4]. The complex dynamics of robotic manipulators having inherent uncertainties, dynamic coupling between neighboring links, time-varying inertia, gravity, and nonlinear frictions require efficient controlling to obtain high control performance of rapid dynamic convergence, repeatable accuracy, finite-time stability, smooth control input, and minimal vibration at the desired angle [5].

In general, nonlinear effects such as presliding displacement, backlash hysteresis, Dahl effect, and Stribeck friction are present in every mechanical system. Basically, the Stribeck friction consists of the Coulomb friction, static friction, and viscous friction [6]. Thus, the motorized mechanism is widely affected by these frictions where moving parts make contact with each other, and it is impractical to pay no attention to the control design. Conversely, this severe nonlinearity may degrade the control performance of the closed-loop system.

A variety of control approaches have been designed, such as neural network-based piecewise con-

*. *Corresponding author.*
E-mail addresses: saim.ahmed@szabist.pk (S. Ahmed); imranghous@cuilahore.edu.pk (I. Ghous); farhan.mumtaz@szabist.edu.pk (F. Mumtaz)

doi: 10.24200/sci.2022.57252.5141

tinuous function control To meet effectual control performance under Stribeck frictions [7], adaptive fuzzy control [8], recursive model-free control [9], Sliding Mode Control (SMC) [10–12]. However, some of these schemes rely on the knowledge of the system dynamics or information of uncertain parameters [13]. Moreover, some intelligent learning control methodologies, such as fuzzy logic and neural network control, require complex calculations caused by the weight training processes of intelligent control.

Toward this front, to avoid complicated formulations and estimate unknown system dynamics and uncertainties, the Time Delay Estimation (TDE) can be employed to achieve high control performance and implemented easily. Fundamentally, TDE is an estimation method that originates from Time Delay Control (TDC) theory. In this way, the unknown dynamics and uncertainties of a system are estimated by exploiting the system's delayed dynamics. Thus, the constant time delay is inserted with known system parameters, such as control input and the state derivatives, to obtain delayed unknown dynamics. In literature, TDE has been incorporated with well-known control methodologies, for example, SMC, fuzzy control, neural network control, and intelligent proportional-integral-derivative (iPID) control [14–18] to obtain a precise estimation as well as better control performances.

On the other hand, TDE cannot precisely estimate the unmodeled dynamics because of the TDE estimation error, which is inevitable due to inherent non-smooth frictions and nonlinearities. Therefore, in order to tackle estimation error, TDE is usually used with various control schemes such as adaptive control, neural network control, fuzzy logic, Ideal Velocity Feedback (IVF), and anti-windup schemes [17–21]. TDE estimates the unknown dynamics, and the other schemes suppress the estimation error. As mentioned earlier, the intelligent schemes are complex enough, and the adaptive control may not be estimated to some extent due to its constant tuning gain. Therefore, the TDE scheme is suitable for its simplicity and precise estimation. In this work, TDE is employed to estimate the unmodeled dynamics, and then the other TDE is utilized to deal with the estimation error caused by the Stribeck friction's effect.

SMC is one of the most robust control schemes in control engineering; however, conventional SMC has some drawbacks, such as slow convergence speed, oscillation in control, and singularity [22]. Thus, Terminal Sliding Mode Control (TSMC), fast TSMC, and nonsingular TSMC have been designed to overcome these problems [23–27]. Furthermore, to enhance the TSMC performances, such as robustness and dynamic response, TSMC based on PID (TSMC-PID) has been designed [28]. Moreover, Fractional-Order (FO) control is an arbitrary order of generalized calculus that improves the dynamic response of the controller. Thus, FO has been integrated with TSMC to improve the tracking accuracy and transient response of the closed-loop system [29–32]. Therefore, this work considers fractional-order TSMC-PID with the estimation of uncertain dynamics under Stribeck friction through TDE to design the robust model-free scheme Fractional-Order TSMC (FOTSMC) and Proportional-Integral-Derivative (PID). At the same time, the chattering problem is attenuated by replacing the *sgn* function with the *tanh* function. The main goal of this work can be marked as follows:

1. Unlike the intelligent learning methods, TDE based FOTSMC-PID control scheme under Stribeck friction is proposed to obtain model-free control with finite-time convergence, high precision, and robustness;
2. FOTSMC-PID is utilized to obtain robust and accurate performances, and unknown dynamics are estimated by TDE. In contrast, TDE error is compensated by integrating augmented control via another TDE approach;
3. A proof of finite-time stability is investigated by Lyapunov stability synthesis;
4. The proposed scheme shows a faster convergence rate and robustness with compared approaches.

The article is organized as follows: Mathematical preliminaries are given in Section 2. Section 3 introduces the dynamics of robotic manipulators. In Sections 4 and 5, the proposed TDE framework with FOTSMC-PID for robotic manipulators and its finite-time stability analysis by Lyapunov synthesis is demonstrated, respectively. Section 6 presents the resultant comparative simulations to validate the efficacy of the developed scheme. This paper is concluded in Section 7.

2. Mathematical preliminaries

2.1. Definition 1

A perturbed nonlinear system with state $z(t)$ is defined as:

$$\dot{z}(t) = g(z) + h(z)u(t) + p(t), \tag{1}$$

where $g(z)$ represents the unknown nonlinear state dynamics function, $h(z)$ denotes a distribution matrix, $p(t)$ is an unknown external disturbance, and the control input is given by $u(t)$. By separating known and unknown terms, Eq. (1) can be written as:

$$\Theta(z,t) = g(z) + p(t) = \dot{z}(t) - h(z)u(t). \tag{2}$$

The TDE of an unmodeled term can be computed as [33]:

$$\hat{\Theta}(z,t) \triangleq \hat{g}(z) + \hat{p}(t) \triangleq g_{(z-d)} + p_{(t-d)} = \dot{z}_{(t-d)} - h_{(z-d)} u_{(t-d)}, \quad (3)$$

where d is the constant delay, and $\hat{\Theta}(z,t)$ is the estimated expression of unknown dynamics.

2.2. Definition 2

The γth-order Riemann-Liouville (RL) fractional differointegral of function $z(t)$ with terminal value b is defined by Podlubny [34]:

$${}_b\mathcal{I}_t^{\gamma} z(t) = {}_b\mathcal{D}_t^{-\gamma} z(t) = \frac{1}{\Gamma(\gamma)} \int_b^t \frac{z(\tau)}{(t-\tau)^{1-\gamma}} d\tau, \quad (4)$$

$${}_b\mathcal{D}_t^{\gamma} z(t) = \frac{d^{\gamma} z(t)}{dt^{\gamma}} = \frac{d^{[\gamma]}}{dt^{[\gamma]}} {}_b\mathcal{I}_t^{[\gamma]-\gamma} z(t), \quad (5)$$

where $\mathcal{I}^{\gamma}$ and $\mathcal{D}^{\gamma}$ represent the fractional integral and derivative, respectively. Fractional value γ ranges $m-1 < \gamma < m$ and $m \in \mathbb{N}$, while $\Gamma(\cdot)$ denotes Euler's Gamma function as:

$$\Gamma(\gamma) = \int_0^{\infty} e^{-t} t^{\gamma-1} dt. \quad (6)$$

2.3. Lemma 1

By taking the ordinary derivative (d^n/dt^n) of fractional operator ${}_b\mathcal{D}_t^{\gamma} z(t)$ yields [34]:

$$\frac{d^n}{dt^n}({}_b\mathcal{D}_t^{\gamma} z(t)) = {}_b\mathcal{D}_t^{\gamma} \left(\frac{d^n z(t)}{dt^n} \right) = {}_b\mathcal{D}_t^{\gamma+n} z(t). \quad (7)$$

2.4. Lemma 2

For Lyapunov function $\mathcal{V}(t)$ with initial value $\mathcal{V}(t_0)$, finite-time stability is implied by Tang [35]:

$$\dot{\mathcal{V}}(t) \leq -n\mathcal{V}^p(t), \quad \forall t \geq t_0, \ \mathcal{V}(t_0) \geq 0, \quad (8)$$

where $n > 0$ and $0 < p < 1$. The finite-time t_f can be estimated as:

$$t_f \leq \frac{1}{n(1-p)} \mathcal{V}^{1-p}(t_0). \quad (9)$$

3. Dynamics of robotic manipulators

The uncertain dynamics of n-link robotic manipulators can be expressed in the Lagrange form as:

$$M(q)\ddot{q} + V_c(q,\dot{q})\dot{q} + G(q) + \mathcal{F}(\dot{q}) + \tau_d = \tau, \quad (10)$$

where $q, \dot{q}, \ddot{q} \in \Re^n$ represents the joints' position, velocity, and acceleration vectors, respectively, the inertia matrix is given by $M(q) \in \Re^{n\times n}$, the Coriolis/centripetal matrix is denoted by $V_c(q,\dot{q}) \in \Re^{n\times n}$, the gravitational vector is represented by $G(q) \in \Re^n$, time-varying unknown external disturbance is denoted by $\tau_d \in \Re^n$, and the control torque is symbolized by $\tau \in \Re^n$. Moreover, the Stribeck friction model can be expressed as [7]:

$$\mathcal{F}(\dot{q}) = \left[\beta_0 + \beta_1 e^{-\psi_1 |\dot{q}|} + \beta_2 (1 - e^{-\psi_2 |\dot{q}|}) \right] sgn(\dot{q}), \quad (11)$$

where $\mathcal{F}(\dot{q}) \in \Re^n$ represents Stribeck friction force, β_0 denotes the Coulomb friction, $(\beta_0 + \beta_1)$ represents the Static friction, β_2 is the Viscous friction coefficient, and ψ_1 and ψ_2 are positive constants.

3.1. Assumption 1

The $M(q)$ is a uniformly positive definite matrix such that:

$$\lambda_1 I \preceq M(q) \preceq \lambda_2 I, \quad (12)$$

where $\lambda_1 > 0$ and $\lambda_2 > 0$ are constants.

System (10) can be rewritten in the following form as:

$$\ddot{q} + \alpha^{-1}[M(q)\ddot{q} - \alpha\ddot{q} + V_c(q,\dot{q})\dot{q} + G(q) + F(\dot{q}) + \tau_d] = \alpha^{-1}\tau. \quad (13)$$

Then Eq. (13) can further be simplified as:

$$\ddot{q} = \alpha^{-1}\tau + \mathcal{M}(q,\dot{q},\ddot{q}), \quad (14)$$

where α is a constant diagonal matrix and:

$$\mathcal{M}(q,\dot{q},\ddot{q}) = -\alpha^{-1}[M(q)\ddot{q} - \alpha\ddot{q} + V_c(q,\dot{q})\dot{q} + G(q) + F(\dot{q}) + \tau_d].$$

Now, we can represent Eq. (14) in the tracking error form as:

$$\ddot{\tilde{q}}(t) = \alpha^{-1}\tau + \mathcal{M}(q,\dot{q},\ddot{q}) - \ddot{q}_d, \quad (15)$$

where $\tilde{q}(t) = q(t) - q_d(t)$, $\dot{\tilde{q}}(t) = \dot{q}(t) - \dot{q}_d(t)$, $\ddot{\tilde{q}}(t) = \ddot{q}(t) - \ddot{q}_d(t)$, and $q_d, \dot{q}_d, \ddot{q}_d \in \mathcal{L}_\infty$ are the desired trajectory vectors.

4. Controller development

In this section, a model-free controller is proposed using TDE with FOTSMC-based PID (FOTSMC-PID) for the uncertain robotic dynamics under Stribeck fiction and external disturbances. Then, the finite-time stability of the closed-loop system is investigated using Lyapunov's theorem analysis.

4.1. FOTSMC-PID surface

The sliding surface, based on the properties of FO and PID, is designed to obtain a fast response, high

robustness, and finite-time convergence under non-smooth friction. Thus, the terminal sliding manifold is defined as:

$$\mathcal{S} = \tilde{q} + \mathcal{K} \int |\tilde{q}|^{\lambda} sgn(\tilde{q}) d\tau, \tag{16}$$

where $\mathcal{K} > 0$ is a diagonal matrix and $1 < \lambda < 2$.

Once the tracking error reaches the sliding surface $\mathcal{S} = 0 (\dot{\mathcal{S}} = 0)$, it guarantees the finite-time convergence of the error $\tilde{q}$; one gets:

$$\begin{aligned} &\tilde{q} + \mathcal{K} \int |\tilde{q}|^{\lambda} sgn(\tilde{q}) d\tau = 0 \\ &\Rightarrow \dot{\tilde{q}} + \mathcal{K} |\tilde{q}|^{\lambda} sgn(\tilde{q}) = 0 \\ &\Rightarrow \dot{\tilde{q}} = -\mathcal{K} |\tilde{q}|^{\lambda} sgn(\tilde{q}). \end{aligned} \tag{17}$$

Consider the positive-definite Lyapunov candidate as $V = \frac{1}{2} \tilde{q}^T \tilde{q}$, which has:

$$\dot{V} = \tilde{q}^T \dot{\tilde{q}}, \tag{18}$$

$$\dot{V} = -\mathcal{K} \tilde{q}^T |\tilde{q}|^{\lambda} sgn(\tilde{q}) \leq -\mathcal{K} \|\tilde{q}\|^{\lambda+1}, \tag{19}$$

$$\dot{V} \leq -\mathcal{K} (2V)^{\frac{\lambda+1}{2}} \leq -\mathcal{K} (2)^{\frac{\lambda+1}{2}} (V)^{\frac{\lambda+1}{2}} \leq -bV^{\beta}. \tag{20}$$

With $\beta = \frac{\lambda+1}{2}$ and $b = \mathcal{K} 2^{\beta}$. According to Lemma 2, the finite-time convergence can be calculated as follows:

$$t_s = \frac{V^{1-\beta}(t_r)}{b(1-\beta)}, \tag{21}$$

where t_s is the settling time, and reaching time t_r will be calculated in Theorem 1.

Using terminal sliding surface Eq. (16), the following FOTSMC-PID sliding surface is developed as:

$$\mathcal{S}_{pid} = \mathcal{K}_p \mathcal{S} + \mathcal{K}_i \mathcal{D}^{\gamma-1} \mathcal{S} + \mathcal{K}_d \dot{\mathcal{S}}, \tag{22}$$

where $\mathcal{K}_p, \mathcal{K}_i, \mathcal{K}_d > 0$ are PID gains diagonal matrix, and $0 < \gamma < 1$ is FO value.

By taking the derivative of Eq. (22), one can obtain:

$$\dot{\mathcal{S}}_{pid} = \mathcal{K}_p \dot{\mathcal{S}} + \mathcal{K}_i \mathcal{D}^{\gamma} \mathcal{S} + \mathcal{K}_d \ddot{\mathcal{S}}. \tag{23}$$

Substituting second derivative of Eq. (16) into Eq. (23) yields:

$$\dot{\mathcal{S}}_{pid} = \mathcal{K}_p \dot{\mathcal{S}} + \mathcal{K}_i \mathcal{D}^{\gamma} \mathcal{S} + \mathcal{K}_d (\ddot{\tilde{q}} + \lambda \mathcal{K} |\tilde{q}|^{\lambda-1} \dot{\tilde{q}}). \tag{24}$$

Substituting $\ddot{\tilde{q}}(t)$ from Eq. (15) into Eq. (24), one has:

$$\begin{aligned} \dot{\mathcal{S}}_{pid} = \mathcal{K}_p \dot{\mathcal{S}} + \mathcal{K}_i \mathcal{D}^{\gamma} \mathcal{S} + \mathcal{K}_d (\alpha^{-1} \tau + \mathcal{M}(q, \dot{q}, \ddot{q}) \\ - \ddot{q}_d + \lambda \mathcal{K} |\tilde{q}|^{\lambda-1} \dot{\tilde{q}}). \end{aligned} \tag{25}$$

The FOTSMC and PID sliding surfaces are merged, and the proposed sliding surface is developed Eq. (22). Therefore, the FOTSMC-PID surface has the advantage of both schemes, for instance, rapid dynamics response, quick finite-time convergence, small steady-state error, and non-singularity. For the uncertain systems, the mentioned properties are elemental because they are robust against uncertainties and parameter variations, and the system stabilizes swiftly.

4.2. TDE with FOTSMC-PID-based model-free control design

In this subsection, the design of the proposed control is presented by combining the schemes such as TDE with the enhanced FOTSMC-PID approach to estimate unknown dynamics of robotic manipulators under frictions and external disturbances. For such a problem of model-free tracking control, the proposed controller is designed as follows:

$$\tau = \tau_{nom} + \tau_{est} + \tau_{aug}, \tag{26}$$

where τ_{nom} is nominal control, and τ_{est} is estimation control by TDE, while τ_{aug} will be discussed later. Here, τ_{nom} and τ_{est} are respectively defined in Eqs. (27) and (28) as:

$$\tau_{nom} = \alpha (\ddot{q}_d - \lambda \mathcal{K} |\tilde{q}|^{\lambda-1} \dot{\tilde{q}} - \mathcal{K}_d^{-1} \mathcal{K}_p \dot{\mathcal{S}} - \mathcal{K}_d^{-1} \mathcal{K}_i \mathcal{D}^{\gamma} \mathcal{S}), \tag{27}$$

$$\tau_{est} = -\alpha \hat{\mathcal{M}}, \tag{28}$$

where $\hat{\mathcal{M}}$ denotes TDE, which can be computed by Eq. (14) as:

$$\hat{\mathcal{M}} \triangleq \mathcal{M}(q, \dot{q}, \ddot{q})_{(t-\psi)} = \ddot{q}_{(t-\psi)} - \alpha^{-1} \tau_{(t-\psi)}, \tag{29}$$

where the constant delay ψ and then the delayed term $(t - \psi)$ are obtained.

Thus, by substituting Eq. (26) into Eq. (25), simplified sliding surface is obtained as:

$$\dot{\mathcal{S}}_{pid} = \mathcal{K}_d \left[\alpha^{-1} \tau_{aug} + \tilde{\zeta} \right], \tag{30}$$

where $\tilde{\zeta} = \mathcal{M}(q, \dot{q}, \ddot{q}) - \hat{\mathcal{M}}$. Since the estimation error $\tilde{\zeta}$ does not precisely converge to zero due to hard nonlinearities. Thus, to deal with this situation, τ_{aug} is designed by:

$$\tau_{aug} = -\alpha \left[{\mathcal{K}_d}^{-1} \mathcal{K}_1 sgn(\mathcal{S}_{pid}) + \hat{\tilde{\zeta}} \right], \tag{31}$$

where $\hat{\tilde{\zeta}} \cong \tilde{\zeta}_{(t-\psi)} = \mathcal{K}_d^{-1} \dot{\mathcal{S}}_{pid} - \alpha^{-1} \tau_{aug_{(t-\psi)}}$ is formulated using TDE of Eq. (30) and $\mathcal{K}_1 > 0$.

By substituting Eq. (31) into Eq. (30), one can get:

$$\Longrightarrow \dot{\mathcal{S}}_{pid} = -\mathcal{K}_1 sgn(\mathcal{S}_{pid}) - \dot{\tilde{\zeta}}, \tag{32}$$

where $\dot{\tilde{\zeta}} = \dot{\hat{\tilde{\zeta}}} - \dot{\tilde{\zeta}}$. The complete proposed model structure is shown in Figure 1.

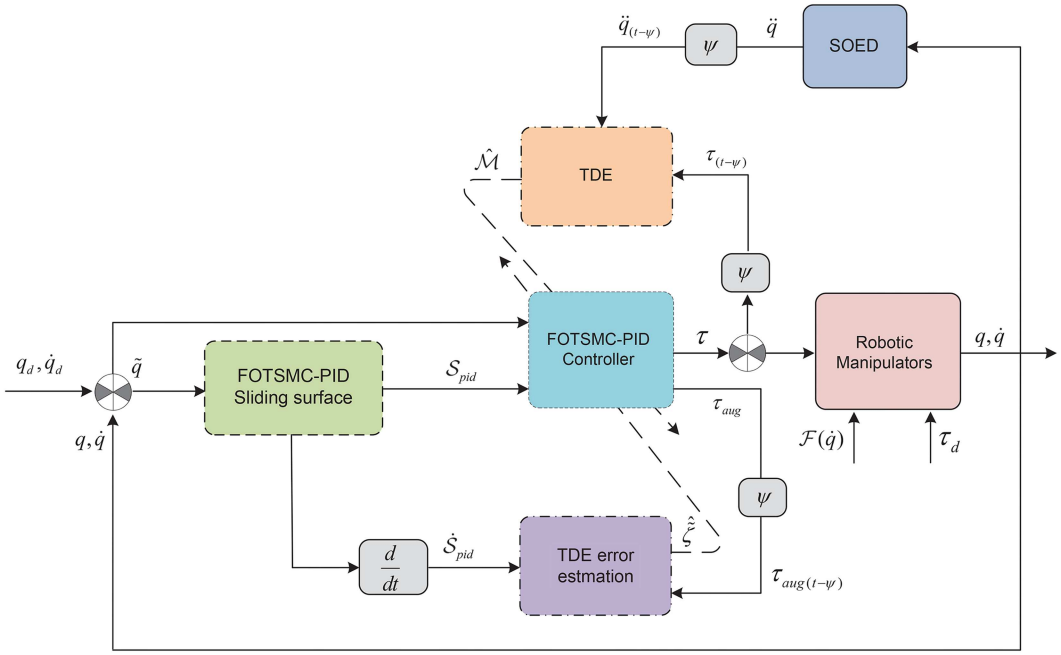

Figure 1. The complete structure of the proposed method.

Remark 1: The proposed FOPID-SMC has four major parameters in comparison with conventional SMC. The first parameter, $\mathcal{K}_p$, helps to sustain the properties of the TSMC. The second parameter, $\mathcal{K}_i$, helps to obtain high robustness properties similar to integral SMC. The third parameter, $\mathcal{K}_d$, helps to obtain chatter-free control input. The fourth parameter, the parameter of FO control γ greatly improves the response of the system. Moreover, the TDE scheme is used to estimate the unknown dynamics of the system.

Remark 2: TDE scheme is applied for an estimation, which means this technique estimates on the basis of delayed parameters/dynamics. For the implementation of the TDE scheme, a sufficiently small delay is used and can be obtained when the sampling period is selected 30 times faster than the controlled system bandwidth [16,36,37].

Remark 3: In the practical implementation of the controller, the acceleration must be known where the position/velocity measurements are available. Thus, the Second-Order Exact Differentiation (SOED) approach can be exploited to estimate the acceleration, which is given as follows:

$$\begin{aligned}
\dot{y}_1 &= -\delta_1 |y_1 - q|^{2/3} sgn(y_1 - q) + y_2, \\
\dot{y}_2 &= -\delta_2 |y_2 - \dot{y}_1|^{1/2} sgn(y_2 - \dot{y}_1) + y_3, \\
\dot{y}_3 &= -\delta_3 sgn(y_3 - \dot{y}_2),
\end{aligned} \tag{33}$$

where $y_1 = q, y_2 = \dot{q}, y_3 = \ddot{q}$ and $\delta_1, \delta_2, \delta_3 > 0$.

5. Stability analysis

The stability synthesis of the developed scheme is carried out by the following theorem.

5.1. Theorem 1

The states of the unknown system under Stibeck friction (11) converge to zero along the manifold $\mathcal{S}_{pid} = 0$ if the designed controller FOTSMC-PID (26) is applied, then it ensures the finite-time stability and convergence of the system.

Let $\mathcal{V}(t)$ be a Lyapunov candidate selected as:

$$\mathcal{V}(t) = \frac{1}{2} \mathcal{S}_{pid}^T \mathcal{S}_{pid}. \tag{34}$$

By taking the time derivative of $\mathcal{V}(t)$, one obtains:

$$\dot{\mathcal{V}}(t) = \mathcal{S}_{pid}^T \dot{\mathcal{S}}_{pid}. \tag{35}$$

Substitution of Eq. (32) into Eq. (35), one can get:

$$\dot{\mathcal{V}}(t) = -\mathcal{S}_{pid}^T \left(\mathcal{K}_1 sgn(\mathcal{S}_{pid}) + \tilde{\tilde{\zeta}} \right), \tag{36}$$

According to $\|\mathcal{S}(t)\| = \mathcal{S}(t)^T sgn(\mathcal{S}(t))$ yields:

$$\dot{\mathcal{V}}(t) \leq -\left(\mathcal{K}_1 + \tilde{\tilde{\zeta}} \right) \|\mathcal{S}_{pid}\|. \tag{37}$$

Since the TDE error $\tilde{\tilde{\zeta}}$ is bounded by $|\tilde{\tilde{\zeta}}| \leq \eta$ with $\eta > 0$ [16] and $\tilde{\tilde{\zeta}} \ll \mathcal{K}_1$, one can express the Relation (37) as:

$$\dot{\mathcal{V}}(t) \leq -\mathcal{K}_1 \|\mathcal{S}_{pid}\| \leq 0. \tag{38}$$

Since $\mathcal{K}_1 > 0$, the system (10) will converge to the origin. Hence, the derived Lyapunov analysis shows the

stability of the system is ensured under the proposed control design.

To compute the finite-time convergence, Relation (38) can be expressed as:

$$\dot{\mathcal{V}}(t) \leq -\varrho \mathcal{V}^{1/2}(t) \leq 0, \tag{39}$$

with $\varrho = \sqrt{2}\mathcal{K}_1$. Thus, implementing Lemma 2 on Relation (39), the finite-time t_r can be formulated as:

$$t_r = \frac{2\mathcal{V}^{1/2}(t_0)}{\varrho}. \tag{40}$$

Therefore, the total finite convergence time can be computed using $t_f = t_r + t_s$ as [38]:

$$t_f = \frac{2\mathcal{V}^{1/2}(t_0)}{\varrho} + \frac{V^{1-\beta}(t_r)}{b(1-\beta)}. \tag{41}$$

Hence, the tracking error will converge to the origin in a finite-time t_f, and the trajectory will maintain converging to the surface manifold when $b > 0$ and $\varrho > 0$.

Remark 4: The finite-time and the control torque are dependent on the constant gain $\mathcal{K}_1$, which is explicitly seen that it is proportional to the τ and reciprocal of t_f in Eqs. (26) and (41), respectively. Thus, better tracking performance, fast finite-time response, and overall dynamic stability can be obtained by selecting the appropriate value of $\mathcal{K}_1$.

Remark 5: The parameters of the FOTSMC-PID method have been chosen according to the specified range, such as $\mathcal{K} > 0$, $\mathcal{K}_p > 0$, $\mathcal{K}_i > 0$, $\mathcal{K}_d > 0$, $\mathcal{K}_1 > 0$, $1 < \lambda < 2$, and $0 < \gamma < 1$. If these parameters are not selected within the given range, then there could be a singularity problem, and the stability of the closed-loop system cannot be achieved. Hence, by selecting the suitable parameters, the desired trajectory tracking and closed-loop system stability can be obtained simultaneously.

6. Simulation evaluations

For the applicability of the theoretical results, the performance of the proposed FOTSMC-PID is validated by implementing 3-DOF dynamics of PUMA 560 robotic manipulators under Stribeck friction. The simulations are performed in the Matlab/Simulink environment with a Runge-Kutta solver under 0.001 sec fixed step size. Moreover, to demonstrate the efficacy of FOTSMC-PID, its results are compared with the proposed scheme without PID (FOTSMC) and Adaptive Fractional-Order Nonsingular TSMC (AFONTSMC) [31].

The dynamics of the considered PUMA 560 manipulators, which were developed in [39], are used. Moreover, the parameters of the proposed and compared controllers are given in Table 1. Initial conditions of joint positions are chosen as $q_1(0) = q_3(0) = 0.1$ and $q_2(0) = 0.05$, and the parameters of SOED Eq. (33) are chosen as $\delta_1 = 20$ and $\delta_2 = \delta_3 = 5$. To counteract the chattering problem, the sgn function in Eq. (26) is replaced by the $tanh$ function. Further, the desired inputs are selected as $q_{d_1} = q_{d_3} = 0.2\cos(0.7t) + 0.2\cos(0.5t - 0.2)$ and $q_{d_2} = 0.2\cos(0.5t - 0.2) - 0.2\cos(0.7t)$.

6.1. Case-1 (without stribeck friction)

The proposed method is compared with FOTSMC and AFONTSMC. Thus, simulations of joint position tracking, tracking errors, and control torques without Stribeck friction are depicted in Figures 2–4. Moreover, the Root Mean Square (RMS) results of position errors are illustrated in Table 2.

These results clearly show the high tracking performance of the proposed method in terms of fast convergence speed, quick response, and chatter-free control inputs.

Table 1. Selected control parameters for Fractional-Order TSMC-PID (FOTSMC-PID), Fractional-Order TSMC (FOTSMC), and Adaptive Fractional-Order Nonsingular TSMC (AFONTSMC).

Controller	Parameters	Values
FOTSMC-PID	$\mathcal{K}$	Diag(30,30,30)
	$\mathcal{K}_p$	Diag(0.2,0.2,0.2)
	$\mathcal{K}_i$	Diag(0.2,0.2,0.2)
	$\mathcal{K}_d$	Diag(0.2,0.2,0.2)
	α	Diag(0.77,0.77,0.77)
	γ, ψ, λ, $\mathcal{K}_1$	0.9,0.001,1.9, 100
FOTSMC	$\mathcal{K}$	Diag(200,200,200)
	γ	0.1
AFONTSMC	k_1	Diag(50,50,50)
	k_2	Diag(10,10,10)
	K	Diag(10,10,10)
	α	0.1

Table 2. Comparative tracking error performance for Fractional-Order TSMC-PID (FOTSMC-PID), Fractional-Order TSMC (FOTSMC), and Adaptive Fractional-Order Nonsingular TSMC (AFONTSMC).

Controller	e_{1RMS}	e_{2RMS}	e_{3RMS}	$\sum_1^3 e_i$
FOTSMC-PID	0.0057	0.0036	0.0057	0.015
FOTSMC	0.0029	0.0032	0.0035	0.0096
AFONTSMC	0.0077	0.0112	0.0073	0.0262

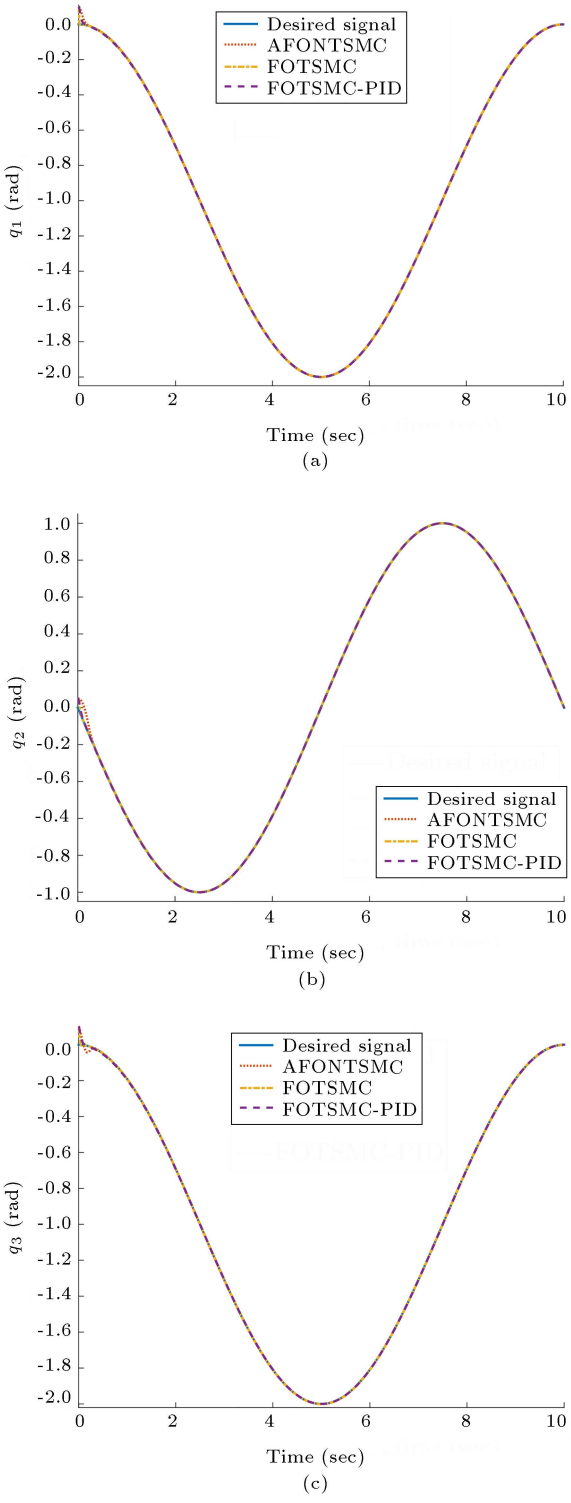

Figure 2. Position tracking for Adaptive Fractional-Order Nonsingular TSMC (AFONTSMC), Fractional-Order TSMC (FOTSMC), and Fractional-Order TSMC-PID (FOTSMC-PID).

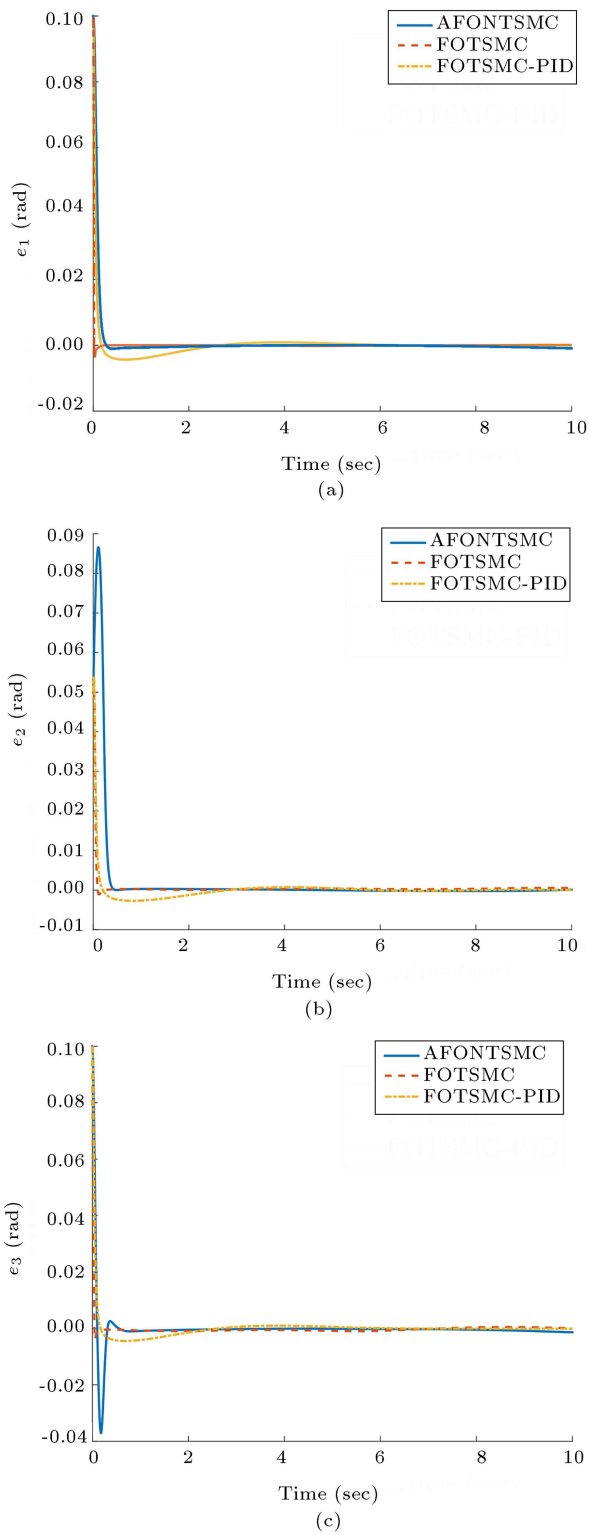

Figure 3. Tracking error for Adaptive Fractional-Order Nonsingular TSMC (AFONTSMC), Fractional-Order TSMC (FOTSMC), and Fractional-Order TSMC-PID (FOTSMC-PID).

6.2. Case-2 (under stribeck friction)

In this case, comparative analyses of the proposed method with FOTSMC and AFONTSMC under Stribeck friction are given. Thus, the Stribeck friction parameters are given as $\beta_0 = 22$, $\beta_1 = 1$, $\beta_2 = 0.96$, $\psi_1 = 55$, and $\psi_2 = 50$. The corresponding comparisons of position tracking, tracking errors, control torques,

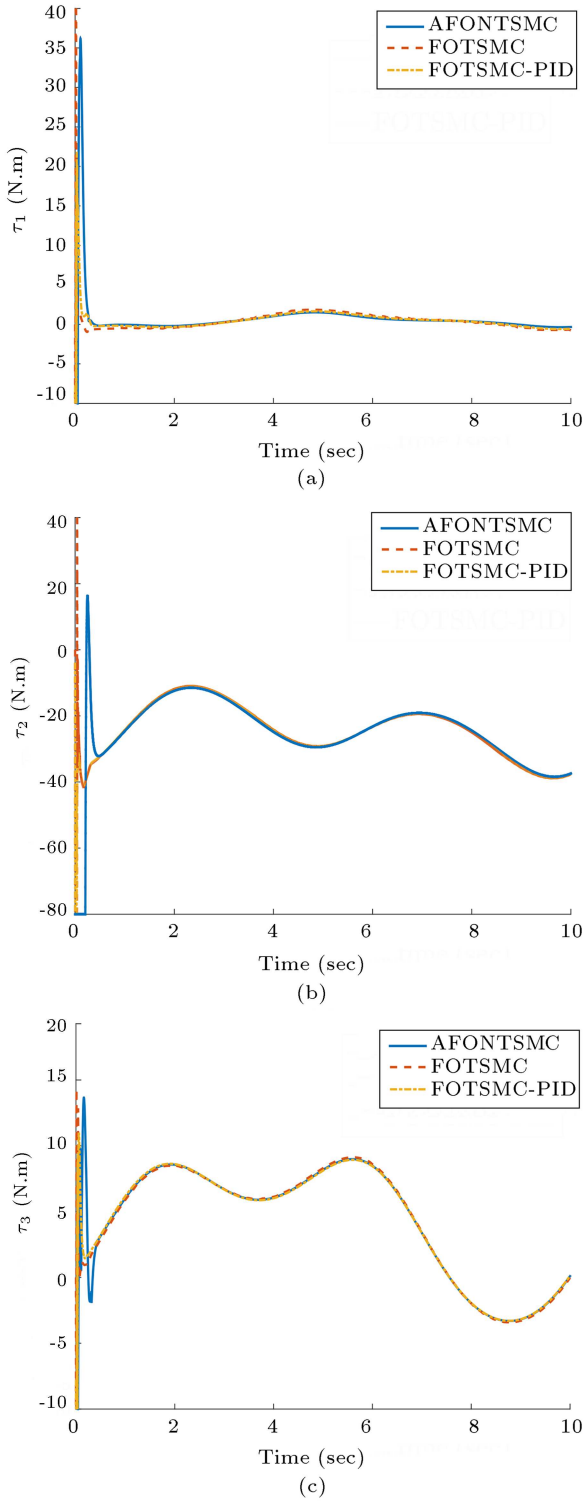

Figure 4. Control torque for Adaptive Fractional-Order Nonsingular TSMC (AFONTSMC), Fractional-Order TSMC (FOTSMC), and Fractional-Order TSMC-PID (FOTSMC-PID).

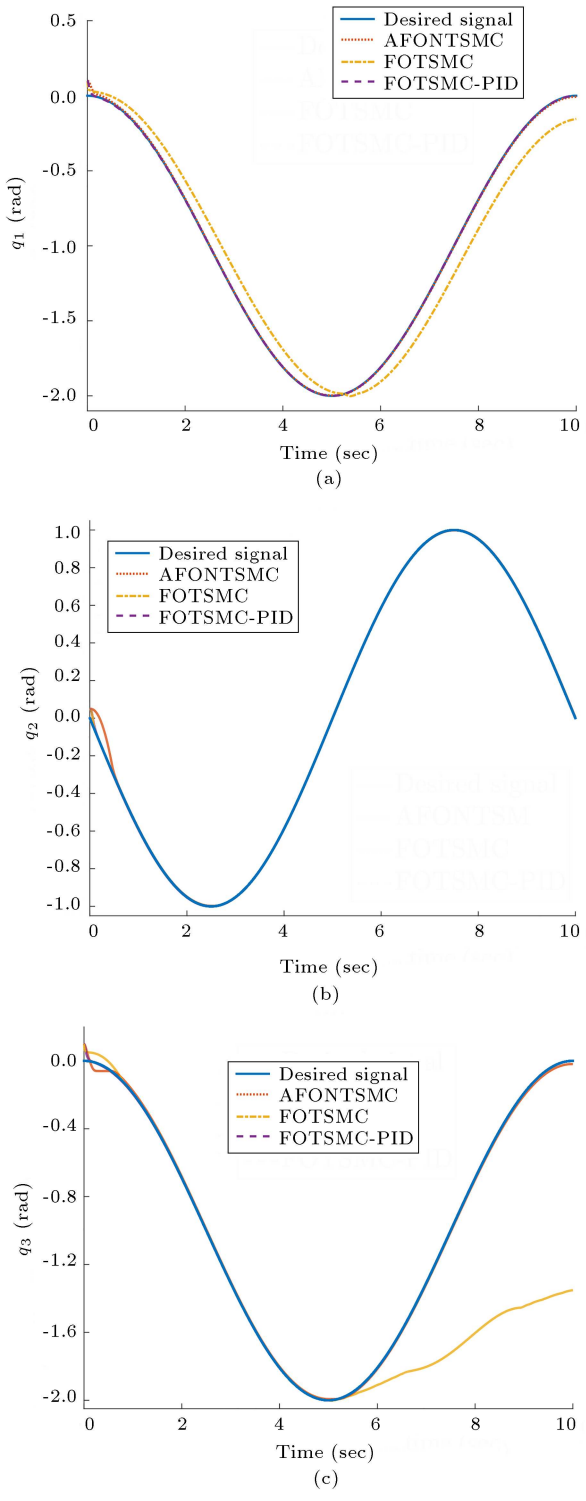

Figure 5. Position Tracking under Stribeck friction for Adaptive Fractional-Order Nonsingular TSMC (AFONTSMC), Fractional-Order TSMC (FOTSMC), and Fractional-Order TSMC-PID (FOTSMC-PID).

and RMS position errors under Stribeck friction are depicted in Figures 5–7 and Table 3, respectively.

According to the results of simulations, Figure 5 depicts the actual joint position of the robotic manipulator and precisely tracks the desired trajectory. Figure 7 shows the satisfactory chatter-free control input performance of the proposed method. Therefore, the comparisons of the proposed method with FOTSMC

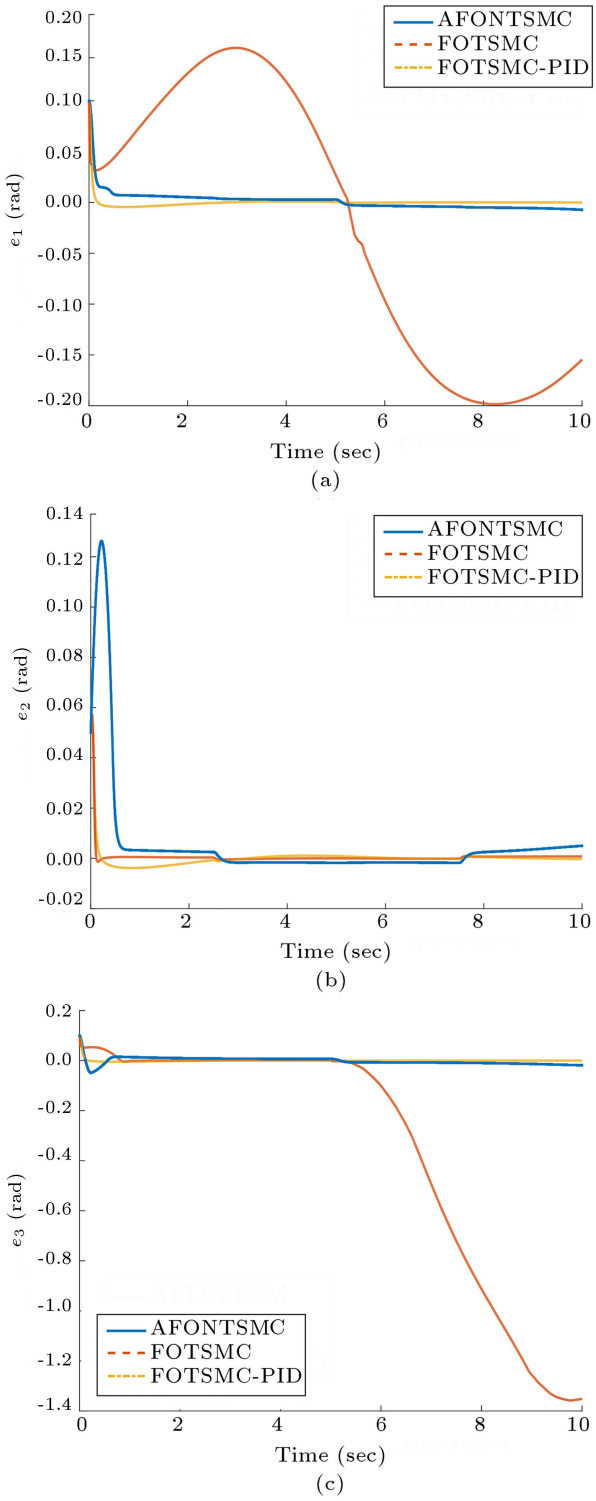

Figure 6. Tracking error under Stribeck friction for Adaptive Fractional-Order Nonsingular TSMC (AFONTSMC), Fractional-Order TSMC (FOTSMC), and Fractional-Order TSMC-PID (FOTSMC-PID).

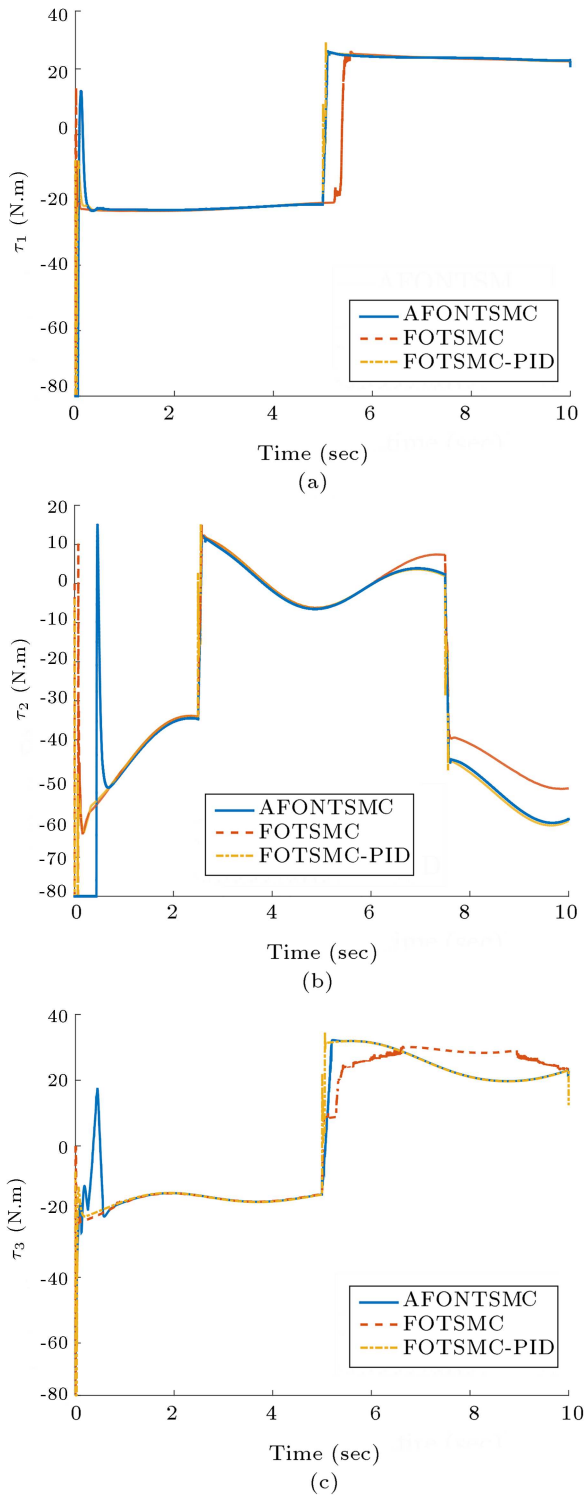

Figure 7. Control torque under Stribeck friction for Adaptive Fractional-Order Nonsingular TSMC (AFONTSMC), Fractional-Order TSMC (FOTSMC), and Fractional-Order TSMC-PID (FOTSMC-PID).

and AFONTSMC show that the performance of all controllers is good without Stribeck friction. As can be seen from Figures 5–7, Stribeck friction considerably affects the dynamics of the robotic manipulator. However, the results under the friction explicitly show that the proposed FOTSMC-PID robustly suppresses the effect of Stribeck friction and obtains effective tracking and fast convergence performances.

Table 3. Comparative tracking error performance under Stribeck Friction for Fractional-Order TSMC-PID (FOTSMC-PID), Fractional-Order TSMC (FOTSMC), and Adaptive Fractional-Order Nonsingular TSMC (AFONTSMC).

Controller	e_{1RMS}	e_{2RMS}	e_{3RMS}	$\sum_1^3 e_i$
FOTSMC-PID	0.0060	0.0048	0.0060	0.0168
FOTSMC	0.1369	0.0043	0.5980	0.7392
AFONTSMC	0.0098	0.0218	0.0138	0.0454

7. Conclusion

A model-free controller based on Time Delay Estimation (TDE) and Fractional-Order TSMC (FOTSMC) and Proportional-Integral-Derivative (PID) is proposed for robotic manipulators under Stribeck friction. Robust dynamic response and precise trajectory tracking are achieved by FOTSMC-PID, whereas unmodeled uncertain dynamics are estimated by TDE. TDE estimation error is generated because of nonlinear friction, which is compensated by designing augmented torque input. Moreover, the developed scheme is equipped with Second-Order Exact Differentiation (SOED) to estimate joint acceleration, which is impracticable to measure. Numerical simulation demonstrates the performance of FOTSMC-PID applied on PUMA 560 manipulators. Moreover, the compared simulation results are illustrated with FOTSMC and Adaptive Fractional-Order Nonsingular Terminal Sliding Mode Control (AFONTSMC), which shows the effectiveness of the proposed scheme.

This paper presents unknown dynamics of the robotic manipulators under Stribeck friction. Therefore, the TDE-based Sliding Mode Control (SMC) approach can be designed to control the system under nonlinearities such as saturation, backlash hysteresis, and dead-zone.

References

1. Yang, L., Wen, R., Qin, J., et al. "A robotic system for overlapping radiofrequency ablation in large tumor treatment", *IEEE/ASME Transactions on Mechatronics*, **15**, pp. 887–897 (2010).
2. Guo, Y., Zhang, S., Ritter, A., et al. "A case study on a capsule robot in the gastrointestinal tract to teach robot programming and navigation", *IEEE Transactions on Education*, **57**, pp. 112–121 (2013).
3. Lukic, M., Barnawi, A., and Stojmenovic, I. "Robot coordination for energy-balanced matching and sequence dispatch of robots to events", *IEEE Transactions on Computers*, **64**, pp. 1416–1428 (2014).
4. Mohan, R.E., Wijesoma, W.S., Acosta Calderon, C.A., et al. "False alarm metrics for human–robot interactions in service robots", *Advanced Robotics*, **24**, pp. 1841–1859 (2010).
5. Ouyang, P., Acob, J., and Pano, V. "Pd with sliding mode control for trajectory tracking of robotic system", *Robotics and Computer-Integrated Manufacturing*, **30**, pp. 189–200 (2014).
6. Márton, L. and Lantos, B. "Control of mechanical systems with stribeck friction and backlash", *Systems & Control Letters*, **58**, pp. 141–147 (2009).
7. Selmic, R.R. and Lewis, F.L. "Neural-network approximation of piecewise continuous functions: application to friction compensation", *IEEE Transactions on Neural Networks*, **13**, pp. 745–751 (2002).
8. Sami, M. and Patton, R.J. "A multiple-model approach to fault tolerant tracking control for nonlinear systems", In *Mediterranean Conference on Control & Automation*, pp. 498–503 (2012).
9. Wang, H., Vasseur, C., and Koncar, V. "Friction compensation of an XY robot using a recursive model free controller", In *International Conference on Industrial Technology*, pp. 355–360 (2010).
10. Soleymani, F., Rezaei, S.M., Rahimi, A., et al. "Multiple-surface sliding mode control of pneumatic actuator with mismatched uncertainties", In *RSI International Conference on Robotics and Mechatronics*, pp. 133–138 (2015).
11. Tsai, Y.-C. and Huang, A.-C. "Multiple-surface sliding controller design for pneumatic servo systems", *Mechatronics*, **18**, pp. 506–512 (2008).
12. Hidalgo, M.C. and Garcia, C. "Friction compensation in control valves: Nonlinear control and usual approaches", *Control Engineering Practice*, **58**, pp. 42–53 (2017).
13. Korayem, M. and Yousefzadeh, M. "Adaptive control of a cable-actuated parallel manipulator mounted on a platform with differential wheels under payload uncertainty", *Scientia Iranica*, **27**, pp. 273–286 (2020).
14. Ahmed, S., Wang, H., and Tian, Y. "Model-free control using time delay estimation and fractionalorder nonsingular fast terminal sliding mode for uncertain lower-limb exoskeleton", *Journal of Vibration and Control*, **24**, pp. 5273–5290 (2018).
15. Wang, H., Ye, X., Tian, Y., et al. "Model-free-based terminal smc of quadrotor attitude and position", *IEEE Transactions on Aerospace and Electronic Systems*, **52**, pp. 2519–2528 (2016).
16. Jin, M., Lee, J., Chang, P.H., et al. "Practical nonsingular terminal sliding-mode control of robot manipulators for high-accuracy tracking control", *IEEE Transactions on Industrial Electronics*, **56**, pp. 3593–3601 (2009).
17. Jin, M., Kim, J., Lee, J., et al. "Improving time-delay control for robot manipulators using tsk fuzzy logic control systems", In *International Conference on Advanced Intelligent Mechatronics*, pp. 1743–1748 (2017).
18. Zhang, X., Wang, H., Tian, Y., et al. "Modelfree based neural network control with time-delay estimation for lower extremity exoskeleton", *Neurocomputing*, **272**, pp. 178–188 (2018).

19. Ahmed, S., Wang, H., and Tian, Y. "Adaptive high-order terminal sliding mode control based on time delay estimation for the robotic manipulators with backlash hysteresis", *IEEE Transactions on Systems, Man, and Cybernetics: Systems*, **51**, pp. 1128–1137 (2019).

20. Jin, M., Kang, S.H., Chang, P.H., et al. "Robust control of robot manipulators using inclusive and enhanced time delay control", *IEEE/ASME Transactions on Mechatronics*, **22**, pp. 2141–2152 (2017).

21. Chang, P.H. and Park, S.H. "On improving timedelay control under certain hard nonlinearities", *Mechatronics*, **13**, pp. 393–412 (2003).

22. Feng, Y., Yu, X., and Man, Z. "Non-singular terminal sliding mode control of rigid manipulators", *Automatica*, **38**, pp. 2159–2167 (2002).

23. Samanfar, A., Shakarami, M.R., Soltani, J., et al. "Adaptive sliding mode control for multi-machine power systems under normal and faulted conditions", *Scientia Iranica*, **29**(5), pp. 2526–2536 (2020).

24. Yu, X. and Zhihong, M. "Fast terminal slidingmode control design for nonlinear dynamical systems", *IEEE Transactions on Circuits and Systems I: Fundamental Theory and Applications*, **49**, pp. 261–264 (2002).

25. Mobayen, S. and Tchier, F. "Nonsingular fast terminal sliding-mode stabilizer for a class of uncertain nonlinear systems based on disturbance observer", *Scientia Iranica*, **24**, pp. 1410–1418 (2017).

26. Torabi, M., Sharifi, M., and Vossoughi, G. "Robust adaptive sliding mode admittance control of exoskeleton rehabilitation robots", *Scientia Iranica*, **25**, pp. 2628–2642 (2018).

27. Bina, M.A., Gitizadeh, M., and Mahmoudian, M. "High-accuracy power sharing in parallel inverters in an islanded microgrid using modified sliding mode control approach", *Scientia Iranica*, **27**, pp. 3128–3139 (2020).

28. Van, M. "An enhanced robust fault tolerant control based on an adaptive fuzzy pid-nonsingular fast terminal sliding mode control for uncertain nonlinear systems", *IEEE/ASME Transactions on Mechatronics*, **23**, pp. 1362–1371 (2018).

29. Ahmed, S., Wang, H., and Tian, Y. "Adaptive fractional high-order terminal sliding mode control for nonlinear robotic manipulator under alternating loads", *Asian Journal of Control*, **23**, pp. 1900–1910 (2021).

30. Wang, Y., Jiang, S., Chen, B., et al. "A new continuous fractional-order nonsingular terminal sliding mode control for cable-driven manipulators", *Advances in Engineering Software*, **119**, pp. 21–29 (2018).

31. Ahmed, S., Wang, H., and Tian, Y. "Fault tolerant control using fractional-order terminal sliding mode control for robotic manipulators", *Studies in Informatics and Control*, **27**, pp. 55–64 (2018).

32. Ahmed, S., Ahmed, A., Mansoor, I., et al. "Output feedback adaptive fractional-order supertwisting sliding mode control of robotic manipulator", *Iranian Journal of Science and Technology, Transactions of Electrical Engineering*, **45**, pp. 335–347 (2021).

33. Youcef-Toumi, K. and Ito, O. "A time delay controller for systems with unknown dynamics", *Journal of Dynamic Systems, Measurement, and Control*, **112**, pp. 133–142 (1990).

34. Podlubny, I., *Fractional Differential Equations: An Introduction to Fractional Derivatives, Fractional Differential Equations, to Methods of their Solution and Some of their Applications*, Academic Press, Elsevier, **198** (1998).

35. Tang, Y. "Terminal sliding mode control for rigid robots", *Automatica*, **34**, pp. 51–56 (1998).

36. Zaare, S. and Soltanpour, M.R. "The position control of the ball and beam system using statedisturbance observe-based adaptive fuzzy sliding mode control in presence of matched and mismatched uncertainties", *Mechanical Systems and Signal Processing*, **150**, 107243 (2021).

37. Zaare, S. and Soltanpour, M.R. "Continuous fuzzy nonsingular terminal sliding mode control of flexible joints robot manipulators based on nonlinear finite time observer in the presence of matched and mismatched uncertainties", *Journal of the Franklin Institute*, **357**, pp. 6539–6570 (2020).

38. Ma, Z. and Sun, G. "Dual terminal sliding mode control design for rigid robotic manipulator", *Journal of the Franklin Institute*, **355**, pp. 9127–9149 (2018).

39. Armstrong, B., Khatib, O., and Burdick, J. "The explicit dynamic model and inertial parameters of the puma 560 arm", In *Proceedings IEEE International Conference on Robotics and Automation*, **3**, pp. 510–518 (1986).

Biographies

Saim Ahmed received his BSc degree in Electronics from Sir Syed University of Science and Technology, Pakistan, in 2009. He received his MSc degree in Industrial Control and Automation from Hamdard University, Pakistan, in 2013. He completed a PhD degree in control science and engineering from Nanjing University of Science and Technology, China, in 2019. He is currently an Assistant Professor at the Department of Mechatronics, Shaheed Zulfikar Ali Bhutto Institute of Science and Technology (SZABIST), Pakistan. His research interests include the theory and applications of adaptive control, sliding mode control, time delay control, robotic exoskeleton and manipulators, nonlinearities, and their compensation.

Imran Ghous received his BSc and MSc degrees in

Electrical Engineering from the University of Engineering and Technology, Taxila, Pakistan, in 2011 and 2013, respectively. He completed his PhD degree in Control Science and Engineering from Nanjing University of Science and Technology, P.R. China, in 2016. He is currently serving as an Assistant Professor at the Department of Electrical and Computer Engineering, COMSATS University Islamabad (Lahore Campus), Pakistan. His research interests mainly include 2-D systems, switched systems, non-linear systems, positive systems, etc.

Farhan Mumtaz received his BSc degree in electronic engineering from Sir Syed University of Engineering & Technology, Karachi, Pakistan, 2012. He received his M.Eng degree from the Department of Electrical Engineering, Hamdard University, Karachi, Pakistan, in 2017. He is currently working as a graduate research assistant in the Department of Electrical and Electronic Engineering, Universiti Teknologi PETRONAS, Perak, Malaysia. He is actively involved in research-based work, with specific research focusing on power electronics and applications.